SANDIA REPORT

SAND2003-8730
Unlimited Release
Printed December 2003

Dynamics of Metal/Ceramic Interface Formation

K. F. McCarty

Prepared by
Sandia National Laboratories
Albuquerque, New Mexico 87185 and Livermore, California 94550

Sandia is a multiprogram laboratory operated by Sandia Corporation,
a Lockheed Martin Company, for the United States Department of Energy's
National Nuclear Security Administration under Contract DE-AC04-94AL85000.

Sandia National Laboratories

Issued by Sandia National Laboratories, operated for the United States Department of Energy by Sandia Corporation.

Available to DOE and DOE contractors from
U.S. Department of Energy
Office of Scientific and Technical Information
P.O. Box 62
Oak Ridge, TN 37831

Telephone: (865)576-8401
Facsimile: (865)576-5728
E-Mail: reports@adonis.osti.gov
Online ordering: http://www.doe.gov/bridge

Available to the public from
U.S. Department of Commerce
National Technical Information Service
5285 Port Royal Rd
Springfield, VA 22161

Telephone: (800)553-6847
Facsimile: (703)605-6900
E-Mail: orders@ntis.fedworld.gov
Online order: http://www.ntis.gov/help/ordermethods.asp?loc=7-4-0#online

SAND2003-8730
Unlimited Release
Printed December 2003

Dynamics of Metal/Ceramic Interface Formation

K.F. McCarty
Materials Physics Department

Sandia National Laboratories
P. O. Box 969
Livermore, CA 94551-0969

ABSTRACT

We summarize the work of the Laboratory Directed Research and Development (LDRD) project "Dynamics of Metal/Ceramic Interface Formation." Low-energy electron microscopy (LEEM) was used to monitor in real time how the metal/ceramic interface between the alloy NiAl and its oxide formed. The interfaces were synthesized by exposing the clean alloy to oxygen at either low or high temperature. During low-temperature exposure, an initially amorphous oxide formed. With annealing, this oxide crystallizes into one type of alumina that has two orientational domains. While the oxide is relatively uniform, it contained pinholes, which coarsened with annealing. In marked contrast, high-temperature exposure directly produced rod-shaped islands of crystalline oxide. These rods were all aligned along the substrate's [001] direction and could be many microns in length. Real-time observations showed that the rods can both grow and shrink by addition and subtraction, respectively, at their ends.

Contents

I. Introduction

In the past decade, considerable effort has been devoted to studying the synthesis of metal/ceramic interfaces. One synthesis approach has been to grow oxide films on metal alloys [1]. This work was partially motivated by needing to understand how such alloys oxidize [2,3]. However, an additional motivation has been to use metal alloys as conducting substrates upon which ordered alumina films can be readily grown. In this manner, model metal/ceramic interfaces and alumina films are produced for studying topics such as ceramic joining, electrical interconnects in microelectronics, supported catalysts, and chemical sensors. In particular, a procedure to make thin, uniform films of crystalline alumina has been developed based upon oxidizing the (110) surface of the ordered intermetallic alloy NiAl [4-8]. The procedure involves exposing the crystal to a large dose (>1000 langmuir, where 1 langmuir = 1 L = 10-6 torr-s) at low temperature (~300°C). The initially amorphous oxide crystallizes upon annealing [5,7,8], forming a layer about 5-Å thick of a phase resembling g-Al2O3 [1,9]. The oxide film is composed of two equally populated domains. Two domains occur because the oxide lattice can fit in two equivalent ways, each being rotated about the surface normal by the same amount but in opposite directions, on the rectangular NiAl (110) surface [6,8].

Here we studied the dynamics of how NiAl forms an oxide interface by oxidation. We imaged the surface in real time using low-energy electron microscopy (LEEM) [10,11]. Two different regimes were investigated – low-temperature oxidation (i.e., the literature recipe of exposing the surface to a high dose of O2 at low temperature followed by annealing at high temperature [7,8] and high-temperature oxidation. During the low-temperature oxidation, we monitor how the amorphous oxide crystallizes into two domains and how these domains grow. Interestingly, we find that pinholes (oxide-free regions) develop when the oxide crystallizes. These regions of unoxidized substrate undergo a coarsening behavior with time and temperature, as do the oxide domains. In addition, we show that the oxidation occurs quite differently if the same procedure is followed except using a lower O2 dose. Then, the oxide incompletely covers the surface and a substantial fraction is not the same oxide type as formed using the high-dose recipe. A completely different metal/ceramic interface forms during the high-temperature oxidation – rod-shaped islands of crystalline oxide form. These rods exhibit fascinating dynamical properties.

II. Experimental

The NiAl (110) crystal was initially cleaned in a preparation chamber coupled to the LEEM vacuum vessel through repeated cycles of sputtering using 500-eV argon ions and annealing at about 900°C, a procedure that produces a well-ordered surface with the same composition as the bulk [12]. The crystal composition was $Ni_{57}Al_{43}$ as measured by wavelength-dispersive electron-microprobe analysis. Temperatures were measured using a W-26%Re/W-5%Re thermocouple that was spot welded to the side of the crystal. The base pressure of the LEEM vacuum chamber was below 10^{-10} torr. Oxygen pressure and doses were measured using an ionization gauge. In the low-temperature oxidation, after imaging a given location on the clean surface, the crystal was exposed to either a high dose or a low dose of O_2 at 325°C. The crystal was then heated to

progressively higher temperatures and the same location was examined using imaging conditions selective to different phases at the surface. In the high-temperature oxidation, the crystal was between 600 and 850°C during oxygen exposure.

Bright-field images [10] were formed from the specular diffraction beam [i.e., the (0,0) reflection] using 3.8 V electrons, a condition that produces dark contrast at the monoatomic steps of the clean NiAl surface. Dark-field imaging conditions were chosen to selectively illuminate just one or the other of the two oxide domains or just the unoxidized NiAl substrate. The oxide domains were imaged at 6.0 V using the (0,2) diffraction spots of each domain (i.e., the second-order spots along the 17.9-Å-long unit-cell axis of each oxide domain [8]). These conditions will be denoted as DF-Ox1 and DF-Ox2, respectively. The oxide-free regions were imaged at 43.5 V using the (0,1) diffraction spot from NiAl (110) (i.e., the first-order spot along the 4.08-Å-long unit-cell axis of NiAl [8]). This condition is denoted as DF-NiAl.

III. Results

Low-temperature oxidation

In the bright-field images of Fig. 1, the dark lines are monoatomic steps on the clean NiAl (110) surface. The dark bands on the right side and in the lower part are step bunches, which serve as spatial fiducials during the high-dose experiment. As this surface at 325°C was exposed to 2 x 10^{-6} torr of O_2, the LEED pattern [7] and the contrast of the steps gradually disappeared. After 1560 L dose, the bright-field images were nearly completely uniform with only slight hints of any contrast at the initial step locations. Consistently, there is no intensity for any of the dark-field imaging conditions, showing that no unoxidized substrate regions (DF-NiAl) or crystalline oxide exist (DF-Ox1 and DF-Ox2). These results are consistent with the previous observations that this magnitude of O_2 dose completely amphorizes the near-surface region [7]. After heating to 695°C, the amorphous oxide has begun to crystallize [7] and some intensity appears in the dark-field conditions specific to the crystalline oxide (see Fig. 2). That is, in images 2a-i and 2b-i, the bright speckles correspond to regions of oxide domain 1 and 2, respectively. With increasing temperature, the fraction of the surface that is crystalline oxide increases as does the size of the oxide domains (see Fig. 2).

The bright speckles of Fig. 3a-i show that oxide-free patches develop when the oxide crystallizes. That is, for the DF-NiAl imaging conditions, intensity only occurs where the substrate is unoxidized. These unoxidized regions are imaged as dark spots in the bright-field images of Fig. 3b. There is a one-to-one correspondence between the dark spots in bright field and the bright spots in dark field. With increasing temperature, the density of unoxidized regions decreases and their size increases. Interestingly, the step bunches serve as sinks for the oxide-free patches. That is, with annealing, the regions adjacent to the step bunches become denuded of oxide-free patches (see locations marked by arrows in images 3a-iii and 3b-iii). Consistently, regions of unoxidized substrate accumulate next to the step bunches.

For the high-dose procedure, Fig. 4 compares surface images obtained at 1015°C using the four different imaging conditions. Away from the step bunches, the two oxide domains together fill the great majority of the surface. However, there are significant patches of unoxidized substrate contained within the interlocked oxide domains. At this temperature, the oxide is decomposing. Interestingly, the oxide-free region grows from the step bunches onto the flatter parts of the substrate.

If the oxide is identically grown except using a much lower dose of O_2, a considerably different film is produced. While the clean starting surface (Fig. 5a) consists mainly of widely spaced steps, there are step bunches on the left and right edges. After exposure to 360 L O_2 at 325°C, the terraces are uniformly illuminated in the bright-field and DF-NiAl conditions, establishing that the oxygen adsorption has occurred uniformly. Figure 5b shows the result after annealing to 925°C. A significant fraction of the surface (the bright regions in the DF-NiAl image 5b-iii) is not covered by oxide. Instead of a uniform film, discrete oxide islands occur on the NiAl terraces and the original NiAl steps are nearly completely decorated by oxide stripes. The DF-Ox1 and DF-Ox2 images, which are formed using diffraction spots unique to the high-dose oxide type, show that the same oxide type also forms on the terraces and decorates the original NiAl steps for this low O_2 dose. Surprisingly, however, much of the oxide does not correspond to either domain of the oxide type made in the standard high-dose procedure. This observation is documented in image 5b-iv, where all the oxide, of any type, on the surface is shaded gray. The black regions, however, mark selectively just the high-dose oxide type. Clearly, a significant fraction of the oxide (the gray regions not overlaid by black regions) is not the high-dose oxide type (the black regions). This establishes that a different type of oxide has formed.

High-temperature oxidation

When the NiAl (110) surface is exposed to oxygen above about 600°C, rod-shaped islands of crystalline oxide form (Fig. 6). These rods are all aligned along the substrate's [001] direction and can be many microns in length. The rods are pseudomorphic with the substrate, as established by selected area diffraction (Fig. 7). Real-time observations show that the rods can both grow and shrink by addition and subtraction, respectively, at their ends. This one-dimensional behavior leads to surprising dynamics. For example, addition at one end and removal at the other end can cause the rods to translate across the surface. A rod can also shrink and totally vanish. In addition, when two rods move close to one another, one rod can grow at the expense of the adjacent rod.

Importantly, we also observed that the rod phase is metastable with respect to the same gamma alumina (γ-Al_2O_3) phase produced by low-temperature oxidation (Fig. 6). That is, eventually islands of the gamma-alumina phase nucleate and grow during the high-temperature oxidation. The γ-Al_2O_3 phase was identified using dark-field microscopy. The γ-Al_2O_3 phase nucleated at steps on the NiAl surface or along the length of the rods. In addition, the γ-Al_2O_3 phase contains strain-relieving interfacial dislocations (120-s image of Fig. 6). These dislocations move with time and we have observed their dynamics. Within an oxide island, the dislocations oscillate back and forth, and the dislocation grows in length as the oxide island grows.

IV. Discussion

Low-temperature oxidation

For the high-dose recipe, the well-characterized crystalline alumina [6-8,13] forms upon annealing. When the oxide has just crystallized, nuclei of both domains are present at high density (see images 2a-i and 2b-i). With time and temperature, the domain density decreases in a coarsening process involving growth of some domains at the expense of others. The resulting structure of interlocked domains is similar to that observed in "mazed" bicrystal films [14]. The driving force causing the coarsening is the reduction in energy that occurs when the boundary length of the domains decreases [15]. Even for temperatures where the oxide is starting to decompose (see images 4a-i and 4a-ii), however, the coarsening is sufficiently inhibited to leave domains of one type completely imbedded in domains of the other type. Furthermore, the boundaries are still rather ragged and have no obvious preferred directions on the NiAl (110) surface.

While the high-dose procedure does produce a relatively uniform film, pinholes do develop when the oxide crystallizes. Even though the surface was given a large O2 dose at elevated temperature, the near-surface region does not incorporate enough oxygen during exposure and/or retain enough oxygen during annealing to produce a complete oxide film of the achieved thickness. The pinholes may occur simply because the amorphous oxide is less dense than its crystalline counterpart. Results from gas adsorption on oxide films prepared by the procedures employed here were used to conclude that the oxide film completely covered the NiAl substrate [7]. However, the present direct-imaging results clearly show that unoxidized regions exist.

The oxide-free areas also probably coarsen because this minimizes the length of the boundaries between the oxide and the unoxidized substrate. The step bunches may act as a sink for the oxide-free areas (images 3a-iii and 3b-iii) just because deposition there reduces boundary length. Alternatively, some other process may be occurring at the steps. However, the coarsening of the unoxidized regions and accumulation at the step bunches clearly show that extensive mass transport of the oxide *compound* is occurring.

For the low-dose oxidation, the oxygen incorporation and retention is far below that needed to make a uniform film. That the original NiAl steps are largely decorated with oxide while the terraces are sparsely covered provides additional support that considerable mass transport occurs during annealing. A surprising observation is the formation of an oxide distinct (the non-overlaid gray regions in image 5b-iv) from the well-characterized type [6-8] made during high-dose oxidation. This new oxide type occurs both at the original NiAl steps and on the terraces. While the low-dose oxide phase is not well characterized, diffraction spots that uniquely illuminate it (but not the high-dose oxide type) in dark-field images were found (see Fig. 5c). This establishes that the phase is crystalline and has well-defined orientational relationships with the substrate. Furthermore, preliminary analysis suggests that two domains of this oxide exists on the NiAl (110) surface. It is possible that the new oxide type observed at low dose is also γ-Al_2O_3, but simply has a different orientational relationship with respect to the substrate than the high-dose oxide. Alternatively, the new oxide produced at low dose may be a different polytype

of alumina [9] or not even alumina at all. Whether the low-dose oxide forms simply because there is less oxygen present or because there is less steric hindrance on the sparsely covered surface is an interesting question. Clearly, though, the NiAl steps influence which oxide type crystallizes. Consider the distribution of oxide phases that decorate the original NiAl step marked by the "**x**" in Fig. 5b-iv. Proceeding clockwise from the "**x**," domain 1 of the high-dose

oxide type first occurs. When the step direction is near the NiAl $[1\bar{1}0]$ direction, the new oxide occurs. When the step is horizontal, domain 2 of the high-dose oxide type is found.

High-temperature oxidation

The effect of temperature on the oxidation of NiAl is dramatic. Oxygen exposure at 350°C gives an amorphous oxide that uniformly covers the surface. In contrast, oxidation above 600°C produces rod-shaped islands of crystalline oxide. The rods are pseudomorphic with the substrate and are all aligned along a unique, principal direction of the substrate. Analysis of NiAl's oxidation by transmission electron microscopy has shown that the spinel NiAl2O4 forms first when the (110) surface is oxidized [4]. The oxygen mesh present on the (111) planes of

NiAl2O4 has a large and small lattice mismatch with the NiAl (110) surface in the $[\bar{1}10]$ and [001] directions, respectively. This is consistent with the rod shape of the island. That is, given

the large strain (28.5%), the NiAl2O4 phase can only grow to a small width in the $[\bar{1}10]$ direction. In the [001] direction, in contrast, the strain is low (1.3%) and the NiAl2O4 phase grows without restraint.

In addition to the rod ($NiAl_2O_4$) phase, γ-Al_2O_3 also forms during high-temperature oxidation. Apparently, there is only a small barrier to nucleating the rod phase – it formed on terraces, well away from steps. The γ-Al_2O_3 phase, in contrast, only nucleated on a substrate step or along the length of a rod. Given that alumina is a more stable oxide than spinel [4], these observations suggest the rod phase is metastable with respect to the alumina phase. That is, the rod phase is kinetically favored (small nucleation barrier) but ultimately unstable to the alumina phase [16].

The alumina phase formed as discrete islands with low density during the high-temperature oxidation. In the islands, linear features were observed, which we interpret as interfacial dislocations. The dislocations formed networks. A commonly observed network was a saw-tooth pattern (Fig. 6), which added "teeth" as the island grew.

V. Summary

In summary, we have used the power of low-energy electron microscopy [10,11] to elucidate how an alloy surface oxidizes at low and high temperature to form a metal/ceramic interface. While the literature recipe [6-8] of oxidizing the NiAl (110) surface using a high O_2 dose at low temperature does produce a relatively uniform film, pinholes develop when the amorphous oxide crystallizes. These regions of oxide-free substrate coarsen, as do the two different domains of oxide, with time and temperature. For a low O_2 dose, the substrate is incompletely covered by a mixture of two different oxides. One oxide type is the well-characterized γ-Al_2O_3 phase [6-8] made at high oxygen dose. The other oxide type is also crystalline and has a well-defined crystallographic relationship with respect to the substrate. High-temperature oxidation is completely different. A crystalline oxide, which we believe is $NiAl_2O_4$, nucleates and grows as rod-shaped islands. The rods are all aligned in one direction. Eventually, at high temperature, islands of γ-Al_2O_3 nucleate at substrate steps or next to the spinel rods. As the γ-Al_2O_3 islands grow, interfacial dislocations develop in the islands and form oscillating networks.

VI. References

[1] R. Franchy, Surf. Sci. Rep. 38 (2000) 199.
[2] D. R. Jennison, C. Verdozzi, P. A. Schultz, and M. P. Sears, Phys. Rev. B 59 (1999) 15605.
[3] A. Y. Lozovoi, A. Alavi, and M. W. Finnis, Phys. Rev. Lett. 85 (2000) 610.
[4] J. Doychak, J. L. Smialek, and T. E. Mitchell, Metall. Trans. A 20 (1989) 499.
[5] H. Isern and G. R. Castro, Surf. Sci. 211 (1989) 865.
[6] K. Müller, H. Lindner, D. M. Zehner, and G. Ownby, Dtsch. Phys. Ges. 25 (1990) 1130.
[7] R. M. Jaeger, H. Kuhlenbeck, H. J. Freund, M. Wuttig, W. Hoffmann, R. Franchy, and H. Ibach, Surf. Sci. 259 (1991) 235.
[8] J. Libuda, F. Winkelmann, M. Bäumer, H. J. Freund, T. Bertrams, H. Neddermeyer, and K. Müller, Surf. Sci. 318 (1994) 61.
[9] K. Wefers and C. Mirsa, Alcoa Tech. Pap. 19 (ALCOA, Alcoa Center, PA, 1987).
[10] E. Bauer, Rep. Prog. Phys. 57 (1994) 895.
[11] M. S. Altman and E. Bauer, Surf. Sci. 347 (1996) 265.
[12] H. L. Davis and J. R. Noonan, J. Vac. Sci. Technol. A 3 (1985) 1507.
[13] J. Wollschläger, Def. Diff. Forum 164 (1998) 37.
[14] N. Thangaraj, K. H. Westmacott, and U. Dahmen, Appl. Phys. Lett. 61 (1992) 37.
[15] Y.-M. Chiang, D. B. Birnie, and W. D. Kingery, Physical Ceramics (John Wiley, New York, 1997), p. 372.
[16] J. Tersoff and R. M. Tromp, Phys. Rev. Lett. 3 (1993) 2782.

FIGURE CAPTIONS

Figure 1: Low-energy electron micrograph of the clean NiAl (110) surface at 325°C before the high-dose oxidation experiment. The field of view (FOV) is 5 mm. The dark lines are monoatomic steps on the alloy surface. The two dark spots, defects in the imaging detector, are fixed to the detector not the sample. The dark bands on the upper right-hand side and the dark semicircle at the bottom are bunches of steps. These bunches serve as fiducials to locate the same region of the substrate throughout the oxidation and during annealing.

Figure 2: LEEM micrographs (FOV = 5 mm) of the NiAl surface after exposure to a "high" dose of O2 (1560 L) at 325°C and annealing to the labeled temperatures. For these dark-field images, the bright regions are where domain 1 (part a, DF-Ox1) or domain 2 (part b, DF-Ox2) of the crystalline g-Al2O3 phase exist, respectively.

Figure 3: LEEM micrographs (FOV = 5 mm) of the NiAl surface after exposure to a "high" dose of O2 (1560 L) at 325°C and annealing to the labeled temperatures.
Part a): Dark-field images (DF-NiAl) where the bright regions show the location of the oxide-free NiAl substrate. With increasing temperature, the oxide-free spots increase in size and their density decreases. In image 3a-iii, there is a distinct denuded zone free of unoxidized patches next to the step bunches, showing that the bunches are sinks for the oxide-free patches.
Part b): Bright-field images, in which the regions of unoxidized substrate appear as dark spots.

Figure 4: LEEM micrographs (FOV = 5 mm) of the NiAl surface after exposure to a "high" dose (1560 L) of O2 at 325°C and annealing to 1015°C. At this temperature the oxide is decomposing, starting next to the step bunches. The same area is examined using four different imaging conditions.

Figure 5: LEEM micrographs of the NiAl surface for the low-dose oxidation experiment.
Part a): Starting (unoxidized) surface (FOV = 5 mm). Except for the step bunches near the left and right edges, the surface is covered by widely spaced single steps.
Part b): After exposure to a "low" dose of O2 (360 L) at 325°C and annealing to 925°C (FOV = 5 mm). A significant fraction of the substrate (the bright regions in the DF-NiAl image, 5b-iii) is not covered by oxide. Image 5b-iv is a composite formed by combining the inverted sum of the two dark-field oxide images (5b-i + 5b-ii) with the dark-field image selective to the unoxidized NiAl surface (DF-NiAl, 5b-iii). In 5b-iv, then, the black-shaded regions show all the oxide of the

type grown by the high-dose recipe. The gray regions shade where any type of oxide occurs. Oxide patches exist both on the terraces and at the original steps that are the same oxide type formed in the high-dose oxidation. However, a significant fraction is a different type of the oxide. Directions on the NiAl (110) surface are drawn on image 5b-ii.
Part c): Different region of the surface after cooling to room temperature. In the bright-field image (5c-i), the features mark where any oxide type occurs. In the composite (DF-Ox1 plus DF-Ox2) of the two dark-field images (5c-ii), the bright regions mark any location of either domain of the high-dose oxide type. Images 5c-iii (20.2 eV) and 5c-iv (49.8 eV) are dark-field micrographs formed from diffraction spots distinct from those of the high-dose oxide type. The three dark-field conditions (5c-ii through 5c-iv) image unique regions of oxide and the sum accounts for all the oxide observed in bright field (5c-i).

Figure 6. LEEM micrographs (5 μm field of view) obtained during the oxidation of the NiAl at 880°C. Initially, "nanorods" of crystalline NiAl2O4 (spinel) islands form and exhibit fascinating dynamics, including translating along the surface. With time "blob-shaped" islands (c) of γ–Al2O3 nucleate either on substrate steps or next to rods. The γ–Al2O3 islands contain linear features that are stress-relieving, interfacial dislocations.

Figure 7. LEEM images and LEED diffraction patterns from the rod oxide phase formed at 750°C in 5×10-8 torr O2. The upper-left image was obtained in bright field, i.e., by forming an image from the specularly reflected (0,0) beam, using 3.8 V electrons. The selected area diffraction patterns (bottom panels) were obtained from the electrons reflected from the surface region within the circle drawn on the bright-field image. In addition to the diffraction spots of the NiAl substrate (marked by black arrows in the 13.5-V LEED pattern), there are streaks along the $[\bar{1}10]$ direction. The upper-right image was obtained by forming an image from a small portion of the streak at the position of the white arrow in the 13.5-eV pattern using 12 eV electrons. Images are 2.5 μm x 2.5 μm. The broad spot in the diffraction patterns results from secondary electrons.

Illustrations

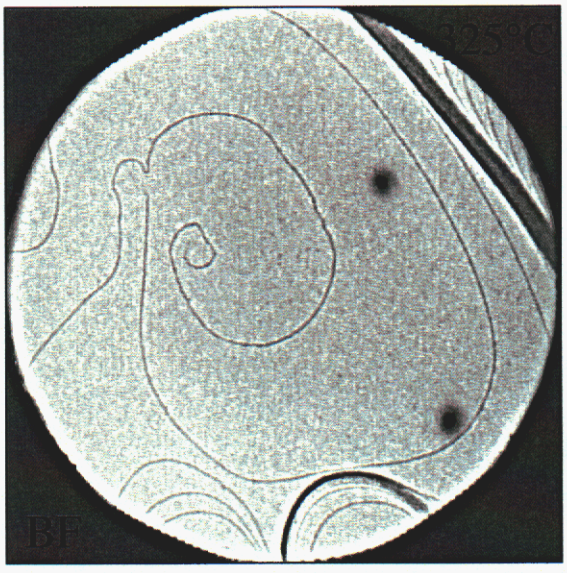

Fig. 1

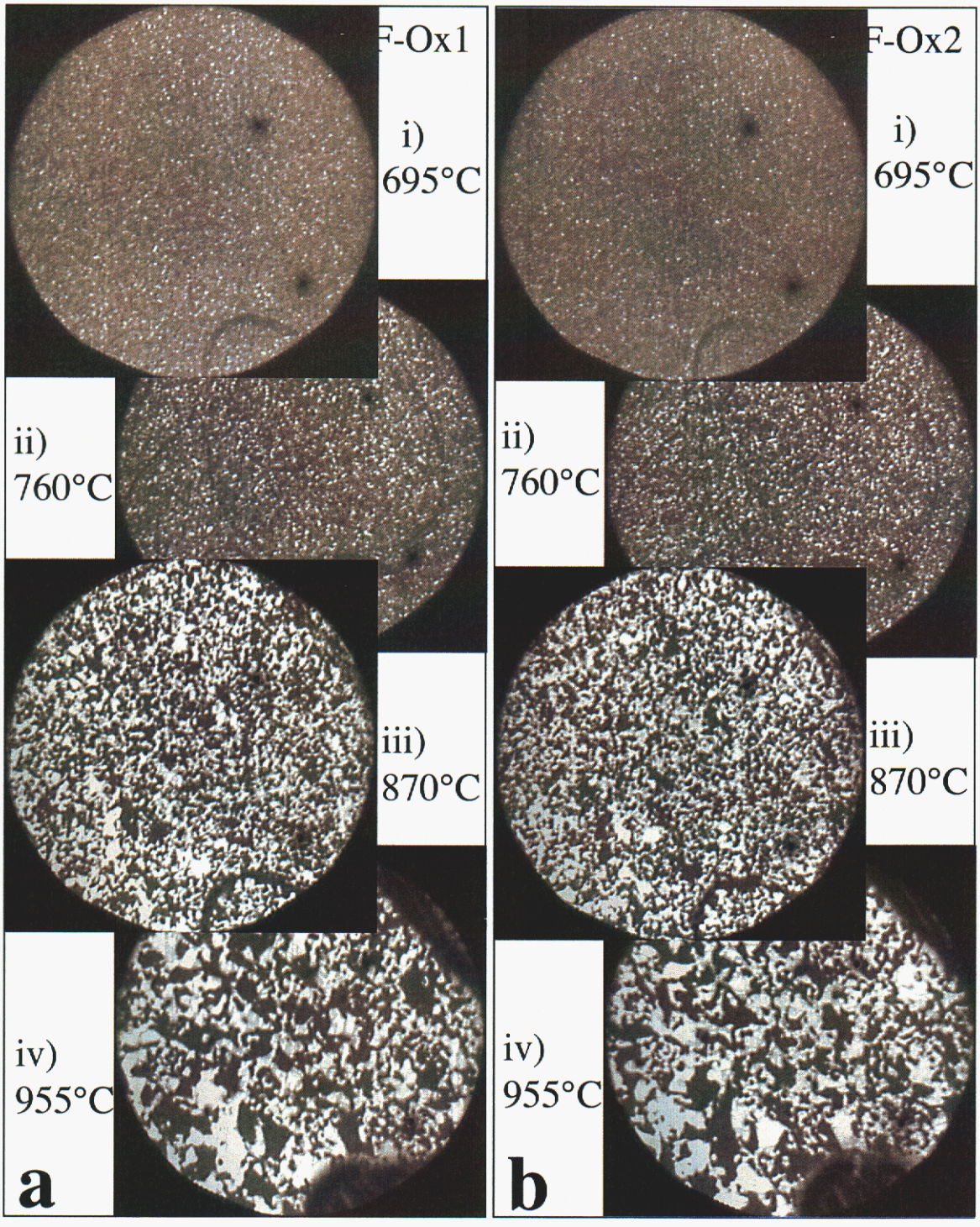
F-Ox1
i)
695°C
ii)
760°C
iii)
870°C
iv)
955°C
a
F-Ox2
i)
695°C
ii)
760°C
iii)
870°C
iv)
955°C
b

Fig. 2

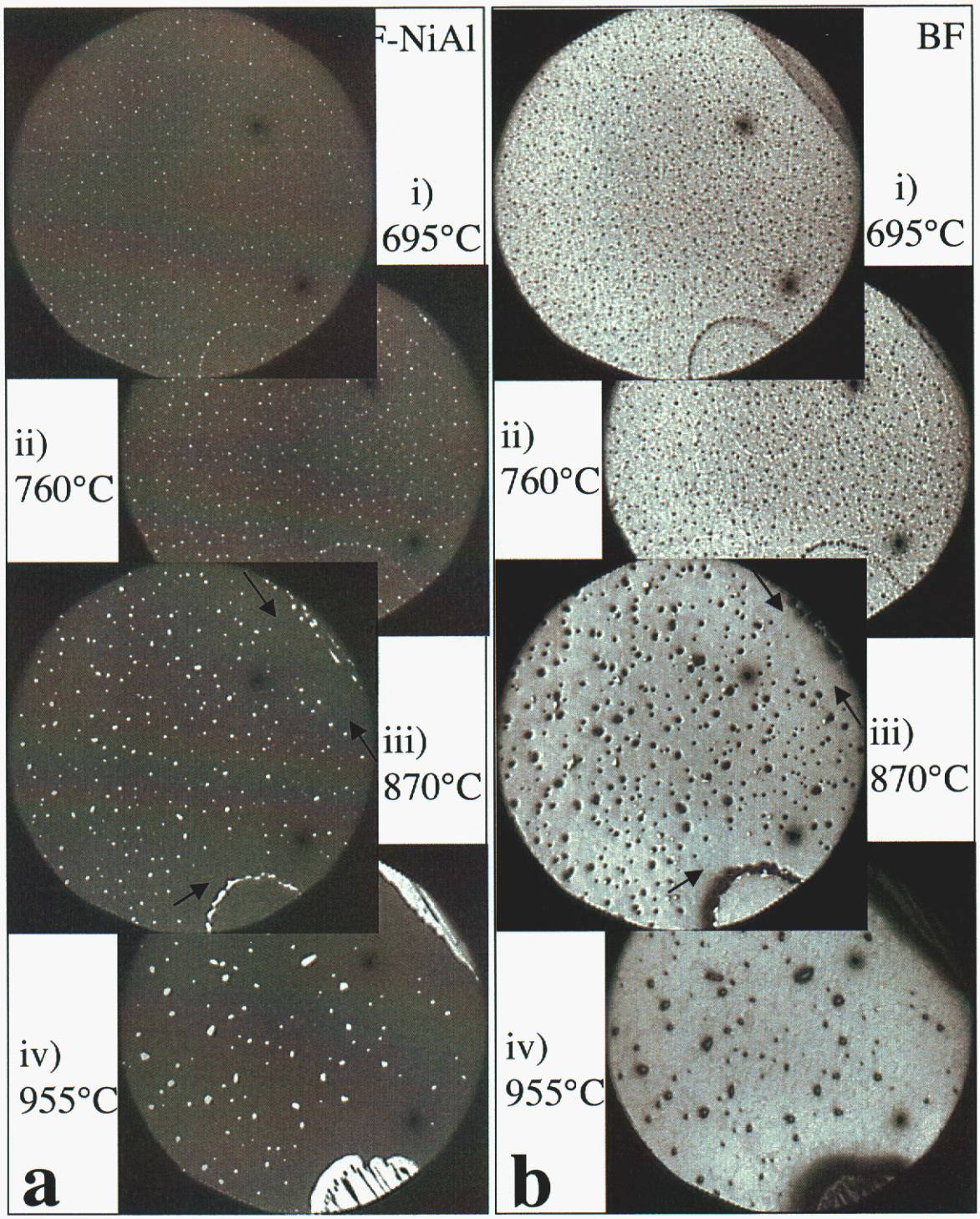
-NiAl
i)
695°C
ii)
760°C
iii)
870°C
iv)
955°C
a
BF
i)
695°C
ii)
760°C
iii)
870°C
iv)
955°C
b

Fig. 3

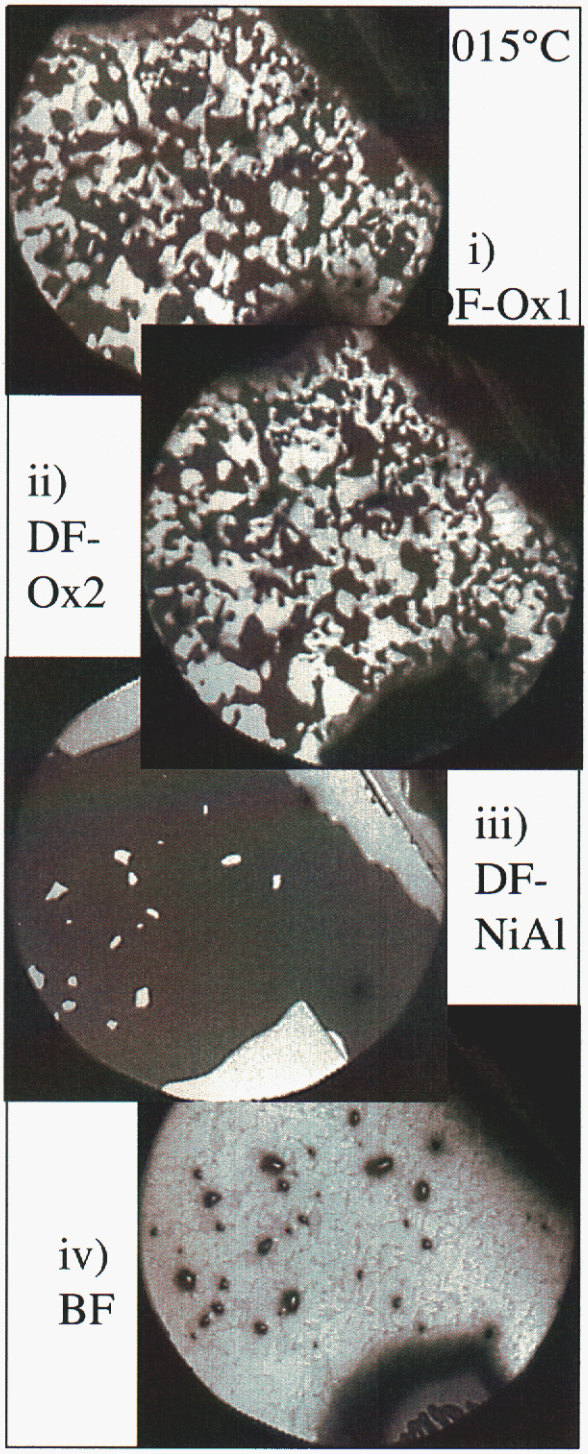

Fig. 4

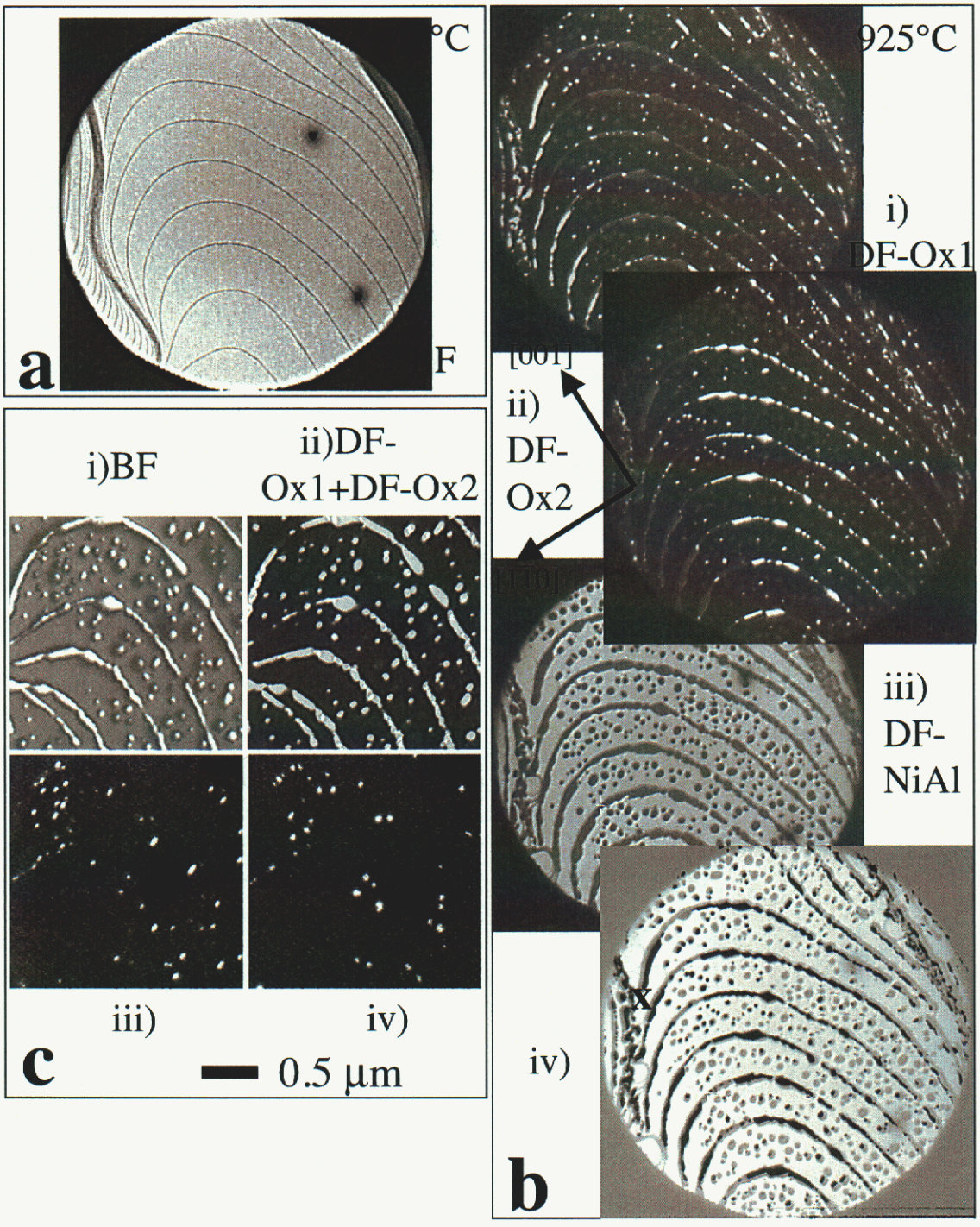
°C
a
F
925°C
i)
DF-Ox1
[001]
ii)
DF-
Ox2
[100]
iii)
DF-
NiAl
iv)
b
i)BF
ii)DF-
Ox1+DF-Ox2
iii)
iv)
c
0.5 µm

Fig. 5

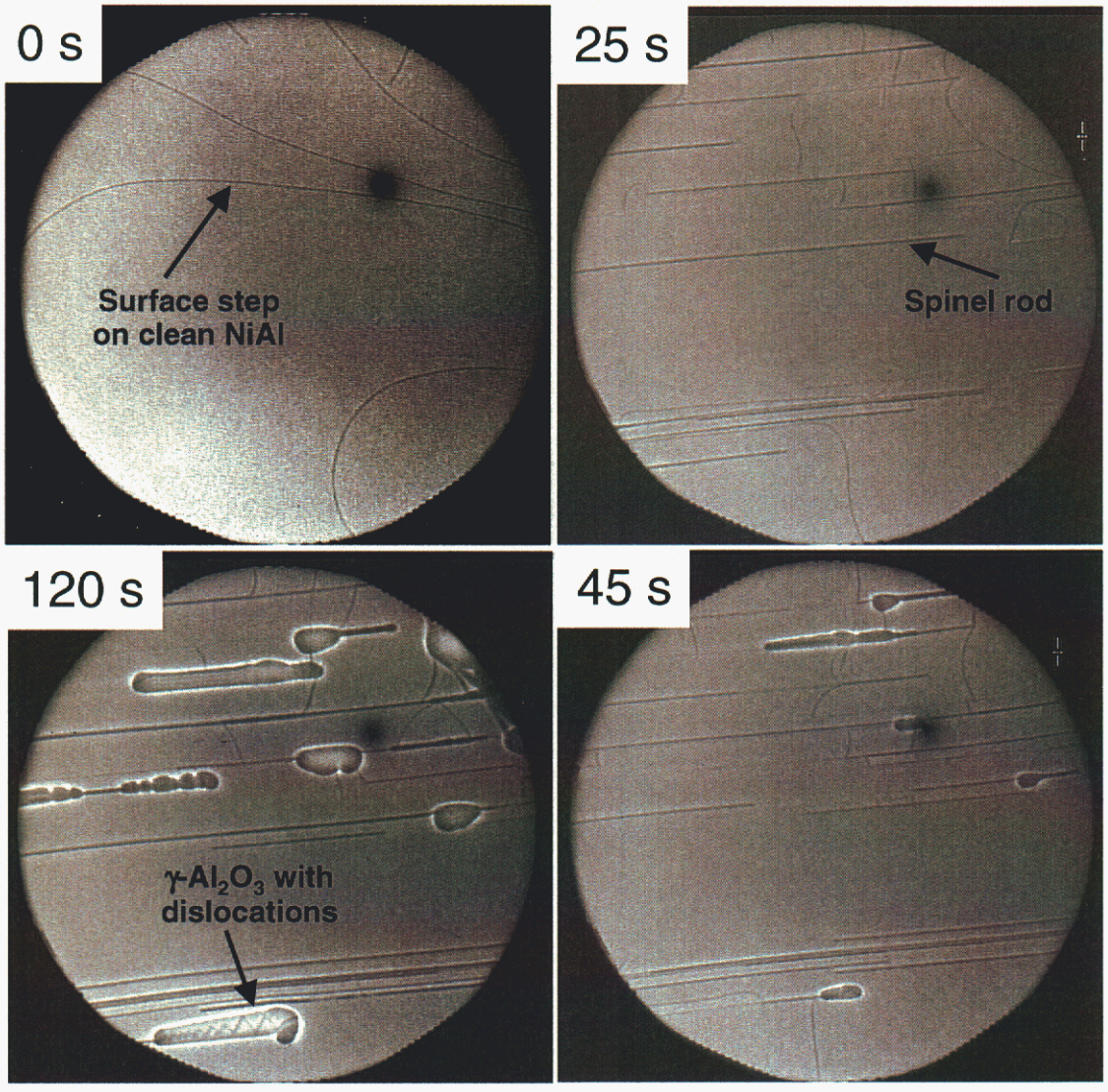
0 s
Surface step
on clean NiAl
25 s
Spinel rod
120 s
γ-Al2O3 with
dislocations
45 s

Fig. 6

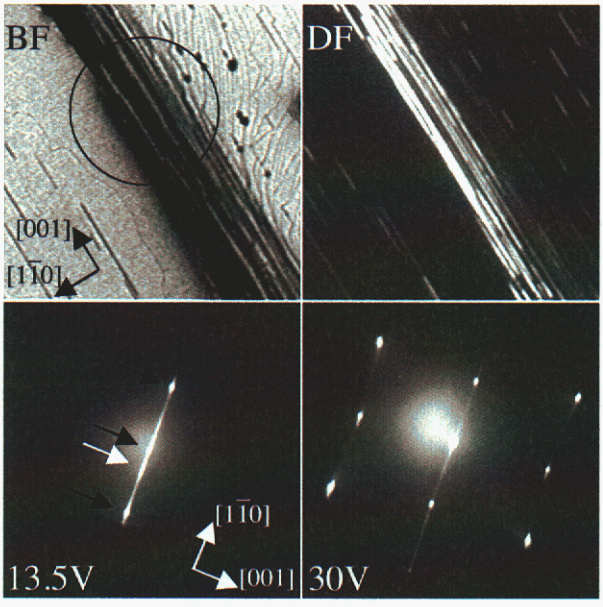

Fig. 7

DISTRIBUTION

1	MS 0323	D. Chavez, LDRD Office, 1001
3	MS 9018	Central Technical Files, 8945-1
1	MS 0899	Technical Library, 9616
1	MS 0612	Classification Office, 8511 for Technical Library, MS 0899, 9616 for DOE/OSTI